Cellular response to linear and branched poly(acrylic acid)

Elizabeth G Whitty, Alison R Maniego, Sharon A Bentwitch, Yohann Guillaneuf, Mark R Jones, Marianne Gaborieau, Patrice Castignolles

DOI: 10.1002/mabi.201500153

Full Paper

Cellular Response to Linear and Branched Poly(acrylic acid) [1]

Elizabeth G. Whitty, Alison R. Maniego, Sharon A. Bentwitch, Yohann Guillaneuf, Mark R. Jones, Marianne Gaborieau*, Patrice Castignolles

E. G. Whitty, A. R. Maniego, S. A. Bentwitch, Dr M. Gaborieau
University of Western Sydney, Molecular Medicine Research Group, Locked Bag 1797, Penrith NSW 2751, Australia
E-mail: m.gaborieau@uws.edu.au

E. G. Whitty, A. R. Maniego, S. A. Bentwitch, Dr M. Gaborieau, Dr P. Castignolles
University of Western Sydney, Australian Centre for Research on Separation Science (ACROSS), Locked Bag 1797, Penrith NSW 2751, Australia

E. G. Whitty, A. R. Maniego, S. A. Bentwitch, Dr M. R. Jones, Dr M. Gaborieau, Dr P. Castignolles
University of Western Sydney, School of Science and Health, Locked Bag 1797, Penrith NSW 2751, Australia

Dr Y. Guillaneuf
Aix-Marseille Université, CNRS, Institut de Chimie Radicalaire, UMR 7273, 13397, Marseille, France

[1] **Supporting Information** is available online from the Wiley Online Library or from the author.

Abstract

Poly(acrylic acid-*co*-sodium acrylate) (PNaA) is a pH-responsive polymer with potential in anticancer drug delivery. The cytotoxicity and intracellular effects of PNaA were investigated, after purification by precipitation or by both precipitation and dialysis, in three branching architectures: 3-arm star, hyperbranched and linear. L1210 progenitor leukemia cells and L6 myoblast cells were chosen as models for cancerous and non-cancerous cells. Simple free solution capillary electrophoresis demonstrated interactions of PNaA with serum proteins and these interactions might be stronger with the more branched architectures. In the MTT assay after 72 h incubation most PNaAs exhibited a IC_{50} between 7 and 14 $mmol \cdot L^{-1}$ in both cell lines, showing that precipitation may be a sufficient purification for PNaA dilute solutions. Dialyzed 3-arm star and hyperbranched PNaA caused an increase in L6 cell viability, challenging the suitability of MTT as cell based cytotoxicity assay for PNaA. Fluorescent confocal microscopy revealed merging of cellular lipids after exposure to PNaA, which was likely caused by serum starvation.

FIGURE FOR ToC_ABSTRACT

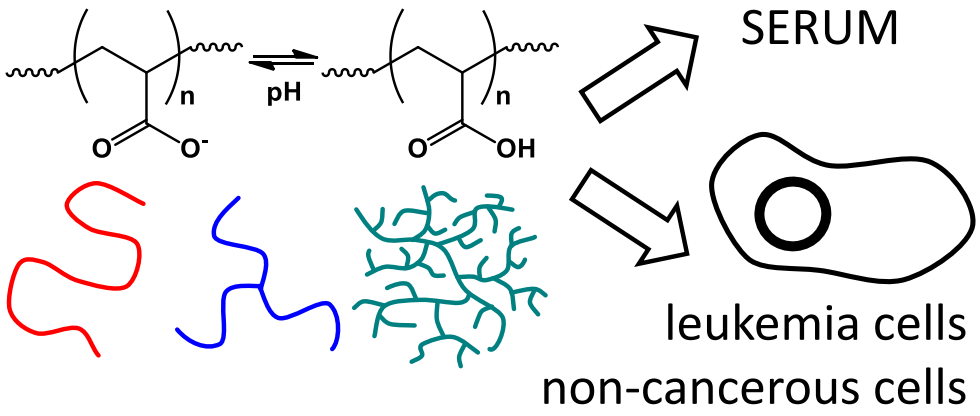

1. Introduction

Polymeric delivery systems are currently in the spotlight of anticancer research to address the harmful side effects commonly associated with anticancer treatment.[1, 2] Ideal drug delivery systems (DDSs) are biochemically non-toxic and inert while encapsulating the drug until it reaches the desired action site.[3] "Smart" polymers, also known as stimuli responsive polymers or environmentally sensitive polymers, are characterized by their ability to respond to changes in the surrounding environment,[4] such as its pH.[5] The main objective of drug targeting is to selectively target tumors by exploiting differences between cancerous and non-cancerous tissues. Cancerous tissues have a lower pH than surrounding tissues (in human and rodent studies, the pH ranges from approximately 5.8 to 7.0 cancerous tissues, while non-cancerous tissues have a pH of approximately 7.5 [6]). pH-responsive polymers such as poly(glutamic acid) and poly(aspartic acid) have been successfully researched for drug delivery [7, 8]. Branched polymers have been found to be suited to drug delivery since they ensure the release of the encapsulated drug in a controlled, prolonged and step-wise manner, as well as no leakage of the drug in water.[9, 10] Branching allows tuning the pK_a, i.e. the pH-responsiveness.[11] Hyperbranched polymers have emerged as a promising candidate for DDSs, as they have a low production cost and require less structural perfection then other potential DDSs such as dendrimers.[12]

Poly(acrylic acid), PAA, is a smart polymer which responds to changes in environmental pH:[13] in alkaline conditions the chemical nature of PAA alters and becomes poly(sodium acrylate) (PNaA). Particles with polystyrene core and PNaA shell exhibited high loading of cisplatin together with a controlled release,[10] thus demonstrating the potential of PAA for cisplatin delivery. PAA can be produced as hyperbranched or star polymers.[14] It is important to test the cytotoxicity of the delivery agent on its own to ensure that no unwanted side

effects like toxicity to non-cancerous cells occur. In this study three architectures (with different branching structures) of PNaA were investigated: a linear, 3-arm star and hyperbranched PNaA. The branching structures of each PNaA corresponds to potential drug loading capabilities which are currently investigated by our team (results not shown); differences in branching structures are not expected to affect cytotoxicity results. Despite PAA's potential as a DDS, literature on its cytotoxicity is scarce. Star with a polystyrene core and a PAA shell were considered not toxic but no data were shown.[10] The few other cytotoxicity studies were performed on PAA as one component in a variety of formulations (e.g. a gelatin based nanoparticle[15], CaF^2:Ce^{3+}/Tb^{3+}-PAA composite microsphere[16] and a PAA terminated silicon nanoparticle[17]). In these previous studies the (branched or linear) molecular architecture of the PAA was not specified [17] and more importantly the cytotoxicity of PAA macromolecules has never been studied independently.[15, 16] Our team recently synthesized and characterized PNaA architectures (linear, 3-arm star, hyperbranched);[14] the cytotoxicity of these PNaAs was assessed for the first time in this work. The non-adherent mammalian B-lymphocyte progenitor L1210 cell line was used as a cancer model and the adherent mammalian myoblast L6 cell line was used as a non-cancerous cell model. The MTT assay assesses cell proliferation and survival to determine cell viability (see SI). In this study the MTT assay was used to assess the in vitro microcytotoxicity of PNaA. The MTT assay is considered by many to be the golden standard of cytotoxicity assays because of its high sensitivity [18].

The interaction of PNaA with serum proteins under physiological conditions has not been previously investigated. Serum and plasma proteins act as conduits for anticancer drugs, enabling intracellular access for anticancer drugs through reversible binding affinities. Determining any effects of PNaA on lipid distribution is useful as it can serve as an early indication that something has in fact entered the cell. The complexation of anticancer drugs to

serum and plasma proteins, mainly transferrin and albumin, are accountable for the delivery and accumulation of anticancer drugs in cancer cells.[19, 20] Free solution Capillary Electrophoresis (CE), or capillary zone electrophoresis (CZE), was shown to be a simple and robust method to characterize the branched structure of PNaA through its electrophoretic mobility.[14] The migration has never been attempted in physiological conditions. The interaction of the polymer with proteins in serum was investigated by CE in this work. While analytical methods such as SEC (size exclusion chromatography, also known as Gel Permeation Chromatography, GPC) were previously favored to analyze protein-drug interactions because of their speed and repeatability,[21] CE is increasingly used as it is faster, robust[22], requires a low sample volume, has superior resolution and the species friendly separation conditions have little impact on the drug-protein integrity during analysis. CE separates drugs from protein-drug conjugates by the differences in their electrophoretic mobility (dependent upon their charge and friction).[23, 24] Replacing electrophoretic mobility shift assays on slab gel, a number of affinity CE methods arose, including Nonequilibrium CE of Equilibrium Mixtures.[25-30]

The identification of specific intracellular structures and the measurement of physiological and biochemical events in living cells is also a very important factor in determining the effect of PAA on cells. Fluorescent confocal microscopy can be used to visualize potential intracellular effects of PNaA. The fluorescent probe Nile Red was used in this study for the in vitro analysis of the effects/interactions of PNaA with serum lipids on the cell membrane and intracellular lipids. Nile Red exhibits emission shifts dependent upon lipid polarity which enables different lipid populations within a cell to be distinguished.[31] The visualization of the effects of PNaA on the cell membrane and intracellular lipids allows for analysis of changes, if any, to the lipid components of cells. The effect of PNaA at a cellular level

requires investigation in order to assess the polymer's biocompatibility and to determine if it negatively interferes with cellular processes.

The aim of this investigation was to assess the cytotoxicity of PNaAs with well-defined branching architectures (linear, 3-arm star and hyperbranched) to both cancerous and non-cancerous cells, as well as to determine the interaction of PNaA with serum proteins under physiological conditions, as part of the assessment of the potential of PNaA as a DDS. The interaction of PNaA with serum as a transport medium for intracellular entry was visualized under confocal fluorescent microscopy with Nile Red staining to observe changes in lipid concentrations in the cell membrane and cytoplasm of L6 cells.

2. Experimental Section

2.1. Materials

Water was of Milli-Q quality. Boric acid (98%) was supplied by BDH AnalaR. Dimethyl sulfoxide (DMSO), sodium hydroxide pellets, sodium bicarbonate Hybri-Max, Nile Red (Nile Blue A Oxazone), trypan blue solution (0.4 %), acetone (99 %) and MTT Formazan powder were supplied by Sigma (Castle Hill, Australia). L6 cells (catalogue number CRL-1458™) and L1210 cells (catalogue number CRL-219™) were obtained from American Type Culture Collection® (ATCC®). Dulbecco's Modified Eagle Medium (DMEM), Fetal Bovine Serum (FBS) (heat-inactivated), sodium pyruvate 100 mM (100 ×), penicillin/streptomycin (5000 $\mu g \cdot mL^{-1}$), Fungizone® (amphotericin B) antimycotic (250 $\mu g \cdot mL^{-1}$), non-essential amino acid solution (100 ×), 2-mercaptoethanol and 0.5% trypsin EDTA (10 ×) were supplied by Life Technologies (Mulgrave, Australia). The linear PNaA sample was supplied by Polymer Standards Service (PSS, Mainz, Germany). The 3-arm star PAA and hyperbranched PAA samples were synthesized by nitroxide-mediated polymerization of

acrylic acid in 1,4-dioxane initiated and controlled by the alkoxyamine BlocBuilder®, which contains the nitroxide SG1 (as per [14]). Sodium borate buffer (110 mM, pH 9.2) was prepared as per [14].

Phosphate Buffered Saline (PBS) (10 mM) was prepared by dissolving 8 g NaCl, 0.2 g of KCl, 1.44 g of Na_2HPO_4 and 0.24 g of KH_2PO_4 in 800 mL of water. pH was adjusted to 7.4 with HCl and final volume was adjusted to 1 L by the addition of water. PBS was sterilized via autoclaving.

2.2. Poly(sodium acrylate) Purification

Precipitation was done in cold diethyl ether. 45 mg of PNaA dissolved at 1 $g \cdot L^{-1}$ in 1 mM NaOH aqueous solution was dialyzed against water using a regenerated cellulose Cellu·Sep® H1 high grade/ultra clean dialysis membrane with a molecular weight cut off < 1000 Da (Membrane Filtration Products Inc.); water was changed daily, 5 times, see **Table 1**.

Table 1. Description of samples and relevant concentrations (in acrylic acid units) used in CE, MTT assay and confocal microscopy.

Sample name	**Dialyzed**	**Moisture content [%]**	**CE concentration [mmol·L^{-1}]**	**MTT concentration [mmol·L^{-1}]**	**Confocal concentration [mmol·L^{-1}]**
Linear PNaA	No	20.44	2 % FBS: 1.5 5 % FBS: 3.6 10 % FBS: 7.3	0.36, 0.90, 1.78, 3.47, 6.63, 9.51, 12.15	2.80
Precipitated 3-arm star PNaA	No	9.42	2 % FBS: 1.7 5 % FBS: 4.2 10 % FBS: 8.3	0.41, 1.02, 2.02, 3.95, 7.54, 10.82, 13.83	3.19
Precipitated hyperbranched PNaA	No	8.44	2 % FBS: 1.7 5 % FBS: 4.2 10 % FBS: 8.4	0.41, 1.02, 2.02, 3.95, 7.54, 10.82, 13.83	3.22
Dialyzed 3-arm star PNaA	Yes	9.42	- [a)]	0.42, 1.04, 2.05,3.99,	- [a)]

				7.62, 10.94, 13.13.98	
Dialyzed hyperbranched PNaA	Yes	8.44	- [a)]	0.42, 1.04, 2.05,3.99, 7.62, 10.94, 13.13.98	- [a)]

[a)] Sample was not tested.

2.3. NMR Spectroscopy

^{1}H NMR spectra for the precipitated and dialyzed PNaAs were recorded using a Bruker DRX300 spectrometer (Bruker Biospin Ltd, Sydney) at Larmor frequency of 300.13 MHz at room temperature. The dialyzed 3-arm star and hyperbranched PNaA were prepared in D_2O (5 g·L^{-1}). The precipitated 3-arm star and hyperbranched PNaA were also prepared in D_2O (30 and 27 g·L^{-1} respectively). ^{1}H NMR spectra were recorded with a 30° flip angle, with a 5 s repetition delay and 128 scans for the precipitated 3-arm star and hyperbranched PNaA, 5 s repetition delay and 256 scans for the dialyzed 3-arm star PNaA and a 10 s repetition delay and 512 scans for the hyperbranched PNaA. The chemical shift scales were calibrated externally with respect to the ethanol signal in D_2O at 1.17 ppm.[32] All experimental data was acquired and processed using Bruker Topspin 1.3 and 3.0 software respectively.

2.4. Thermogravimetric Analysis (TGA)

TGA measurements were carried out on a STA 449 C Jupiter® (Netzsch). The moisture content was measured by heating the samples to 120 ºC under a 25 mL·min^{-1} nitrogen atmosphere using a ramp of 10 ºC·min^{-1} for 10 min; at this temperature an isotherm was kept for 60 min. The percentage of moisture was calculated from the weight lost at the end of the isotherm.

2.5. Capillary Electrophoresis

The instrument and conditions were as in [14] except when stated otherwise. Distributions of electrophoretic mobilities were calculated as in [33]. The fused silica glass capillaries (Polymicro, USA) had a 50 μm i.d., a total length of 62.2 cm (effective length to detection window of 53.7 cm). Serum (FBS) was added to stock solutions of PNaAs at 2 % (v/v), 5 % (v/v) and 10 (v/v), with control serum (FBS) made up to 10 % (v/v) in Milli-Q water.

2.6. Cytotoxicity Assay

L6 cells were seeded in flat-bottomed 96 well microlitre plates and preincubated with growth medium (complete L6 DMEM) overnight (approximately 24 h). L1210 cells were seeded on the day of exposure. L1210 and L6 cells were exposed to different concentrations of PNaA architectures (~0.3 to 14 $mmol \cdot L^{-1}$ of acrylic acid units, see Table 1 for exact values) and incubated for 72 h at 37 °C with 5 % CO_2. Cells were then treated with 20 μL of MTT solution (5 $g \cdot L^{-1}$ dissolved in PBS) and returned to the incubator for 4 h. 170 μL of medium and remaining architectures was subsequently removed (see SI) and 200 μL of DMSO added to each well to dissolve the formazan crystals and the samples were returned to the incubator for 15 min. Absorbance of the converted dye was measured using a spectrophotometer at absorbance wavelength of 540 nm with a reference absorbance wavelength of 690 nm.

2.7. Preparation of Fluorophores and Cell Culture for Confocal Microscopy

A stock solution of Nile Red (1 $mg \cdot mL^{-1}$) was prepared by dissolving Nile Red powder in filter sterilized acetone 99 % (Sigma). The non-adherent mammalian mouse B-lymphocyte progenitor L1210 cell line and the adherent mammalian rat myoblast L6 cell line, obtained from the ATCC®, were studied. Back up cell lines were frozen in 10% (v/v) DMSO/FBS solution. Complete Dulbecco's Modified Eagle Medium (DMEM) was used for the culture of

both L1210 and L6 cells. L6 DMEM contained 2-mercaptoethanol which was absent in the L1210 DMEM. Cells were cultivated and maintained at 37 °C with 5 % CO_2 in a humidified incubator, L6 cells were trypsinized and passaged into fresh complete L6 DMEM every 3-4 days or when they reached a confluency of approximately 80-90 %. L1210 cells were passaged into fresh complete L1210 DMEM every 4-5 days or when they too reached a confluency of approximately 80 – 90 %.

2.8. Laser Scanning Confocal Microscopy

L6 myoblast cells that had reached a confluency of 80-90 % were trypsinised and plated into MatTek plates in 2.5 mL of complete L6 DMEM and left overnight to complete attachment in a 37 °C with 5 % CO_2 humidified incubator. After incubation time, the complete L6 DMEM was removed and the cell monolayer was rinsed three times with 1 mL of incomplete L6 DMEM (to remove excess serum from the FBS present in complete DMEM). 2.5 mL of complete L6 DMEM containing 2 % (v/v), 5 % (v/v) or 10 % (v/v) FBS was added to MatTek plates. L6 cells were exposed to linear PNaA, precipitated 3-arm star PNaA and precipitated hyperbranched PNaA at a concentration of 2.8 and 3.2 $mmol \cdot L^{-1}$ of sodium acrylate units respectively and incubated at 37 °C with 5 % CO_2 for 1 or 24 h. After incubation time cells were exposed to 6.25 µL of Nile Red (concentration added to cells 2.5 $\mu L \cdot mL^{-1}$ in complete DMEM) and left to incubate for 30 min. After incubation period, DMEM was discarded and the cells were washed three times with 1 mL of DMEM containing 2 % (v/v), 5 % (v/v) or 10 % (v/v) FBS respectively to remove any excess Nile Red. Confocal images were acquired with the 488 nm argon laser and the 633 nm HeNe laser.

3. Results and Discussion

3.1. Preparation and Characterization of PNaA

Linear PNaA was obtained by anionic polymerization. 3-arm star and hyperbranched PNaA samples were synthesized by nitroxide-mediated polymerization (NMP)[14] and precipitated to remove impurities. Precipitation was chosen as the most usual and fast purification method. ^{1}H NMR spectroscopy detected residual 1,4-dioxane and sodium acrylate monomers in both 3-arm star and hyperbranched PNaA ([14]and Figure S2).

Some of the 3-arm star and hyperbranched PNaA were then also extensively dialyzed to remove any residual synthesis impurities. The ^{1}H NMR spectra of the PNaAs before and after dialysis are overlaid on Figure S2: the removal of residual 1,4-dioxane and sodium acrylate monomer impurities after dialysis has thus been confirmed. The yield of dialysis was 67.7 % for 3-arm star PNaA and 55.4 % for hyperbranched PNaA, after freeze drying. Thermogravimetric analysis showed a 9.4, 8.4 and 20.4 % water loss in 3-arm star PAA, hyperbranched PAA and linear PNaA respectively (Figure S3). PNaA's moisture content is thus similar to that of other hydrophilic polymers, such as chitosan or starch[34, 35] and consistent with the 3 % moisture of PNaA even after drying.[36] The dialysate was analyzed for traces of PNaA or oligoAA. Both can be detected using CE.[14, 37] Pre-concentration methods allow trace detection.[38] CE with field-amplified sample stacking of dialysate and of membrane rinse showed negligible amounts of oligomers, 1,4-dioxane and acrylic acid monomers present (Figure S1). The cytotoxicity of precipitated and dialyzed samples were compared (see section on cytotoxicity assay) and showed similar cytotoxicities, thus the precipitated samples are the one considered in the rest of the work.

3.2. PNaA-Serum Interactions Probed by Capillary Zone Electrophoresis

Buffers can be used to simulate physiological conditions (pH 7.4) [18, 21, 39] and the CE can maintain the capillary at a constant temperature of 37 °C. CE of the PNaAs at physiological pH in a fused-silica glass capillary was plagued by no recovery (results not shown). It is to be noted that at physiological pH "PNaA" is a copolymer of acrylic acid and sodium acrylate (degree of ionization $\alpha \cong 0.8$, the apparent pK_a of linear PNaA being 6.22 according to [11]). Hydrophobic interactions do not seem to cause the low recovery since CE of PNaA in a capillary coated with a fluorinated polymer (μSiL-FC) led to some recovery but with limited repeatability of migration times (see Figure S4). CE in a capillary coated with poly(ethylene oxide) (μSiL-WAX) under physiological conditions (10 mM sodium phosphate buffer, pH 7.4 at 37 °C) led to repeatable, but poorly reproducible migration times (Figure S5) (the reproducibility corresponding here to different μSiL-WAX capillaries on different days). Adsorption onto the capillary wall[40] was confirmed by strong tailing observed in pressure mobilization experiments with the PNaAs at physiological pH (see Figure S6).

Nonequilibrium CE of Equilibrium mixtures (NECEEM) has however already been performed at pH 9.2 in sodium borate.[28] CE separations in borate buffer at pH 9.2 as per [14] were tested and found repeatable for PNaA and serum proteins. Both serum proteins and PNaA are present only in the sample plug and not in the background electrolyte (as in a NECEEM experiment). PNaA and the proteins of the serum are completely separated (black and green electropherograms on **Figure 1** and Figure S-7). A peak attributed to the complex is clearly detected with an intermediate mobility for the hyperbranched PNaA: the complex has a mobility around 3.4×10^{-8} $m^2.V^{-1}.s^{-1}$ for low (2 %) serum content and it decreases to mobilities closer to that of the proteins, $2.7\text{-}2.8 \times 10^{-8}$ $m^2.V^{-1}.s^{-1}$ for higher protein content (see top left insert). This might be due to different stoichiometry of the complexes depending on the serum to hyperbranched PNaA ratio. In the case of the 3-arm start PNaA, the peak

attributed to the complex is far less intense: it is not observed at 2 % serum and it is weak at the two higher serum contents. Finally in the case of the linear PNaA, no complex is detected. When the PNaA incubated with serum is injected a slight increase in electrophoretic mobility of the free PNaA peak is observed compared to free PNaA. This is observed for the three different PNaA architectures, and this mobility increased with increasing serum content (see top right insert of Figure 1 and Figure S7). This might simply be due to longer migration times due to increasing viscosity of the medium. No tailing of the PNaA peak (no bridge between the PNaA and the complex peak) is observed when the complex are injected contrary to what is typically observed in the case of proteins-DNA complexes:[24, 26, 30] this may indicate that the proteins-PAA complexes dissociate very slowly on the timescale of the migration. It is not possible to extract binding constants since the binding constants would be different with the different proteins composing the serum: spatial separation of the different complexes will be needed [41]. In capillary zone electrophoresis, The following qualitative information is thus obtained: (i) PNaA and proteins are forming a complex at physiological pH that remains at least in part at pH 9.2 (as shown by peak at approximately 2.8×10^{-8} $m^2.V^{-1}.s^{-1}$ in the purple and fuchsia electropherograms), (ii) the change of electrophoretic mobility when PNaA is injected with or without serum also indicates that prior to injection there is an interaction between PNaA and serum proteins (peak at 3.7 to 4×10^{-8} $m^2.V^{-1}.s^{-1}$ in black vs orange, purple, fuchsia electropherograms). The binding of PNaA and serum proteins is likely to affect the activity and mode of action of PNaA as an anticancer DDS. The pharmacological action of anticancer drugs when complexed with PNaA may also be altered.

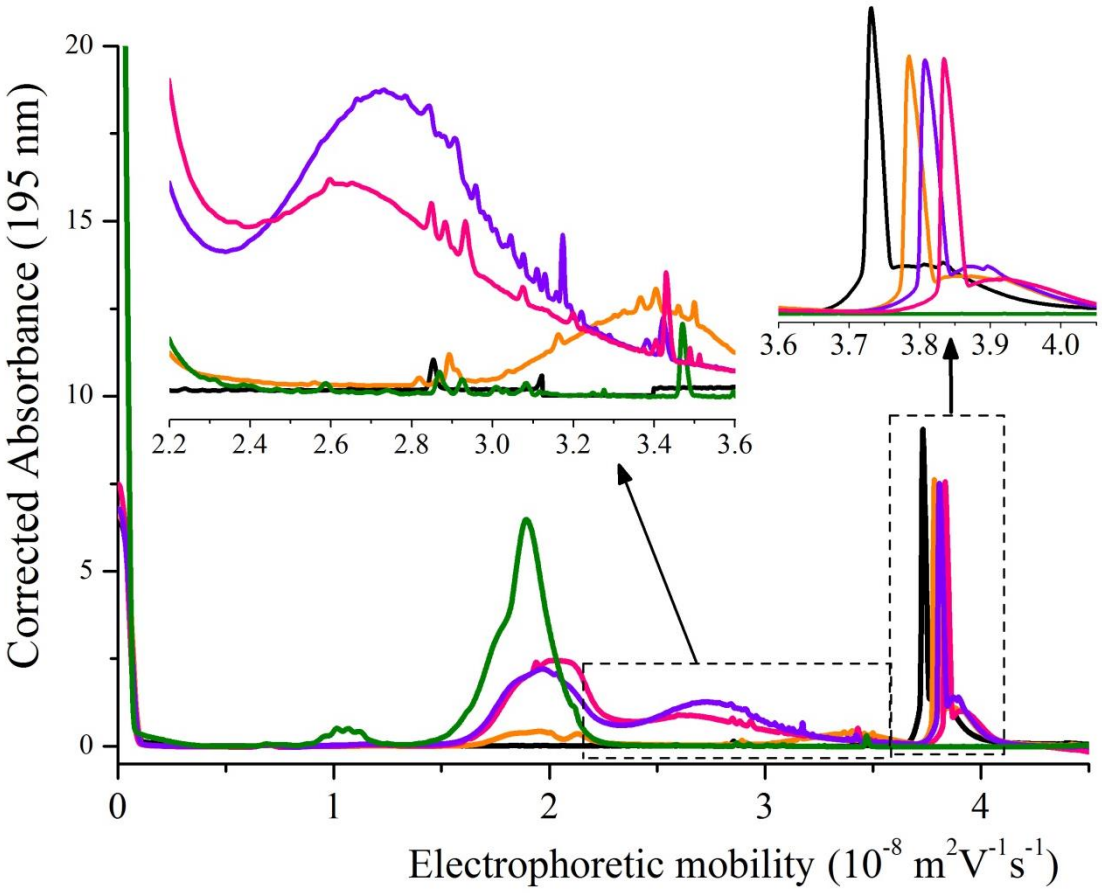

Figure 1. Electropherogram of precipitated hyperbranched PNaA mixed with with FBS: hyperbranched PNaA (black), FBS at 10 % (green), hyperbranched PNaA-FBS 2 % (orange), hyperbranched PNaA-FBS 5 % (purple) and hyperbranched PNaA-FBS 10 % (fuchsia). Insert shows the electrophoretic mobility of hyperbranched PNaA.

Previous studies have found the interaction between bovine serum albumin (BSA) and PAA at pH 6-7 to be weak.[42, 43] BSA has an isoelectric point (pI) of 4.9.[43] In this condition the globules of BSA and the polyions of PAA are negatively charged and their pre-existing electrostatic repulsive forces between PAA and BSA prevent the formation of stable PAA complexes of BSA. These conditions are matched in our experiments with FBS having a pI range of 4.2-3.5 [44] and weak interactions observed at physiological pH.

3.3. Cytotoxicity Assay

Cytotoxicity was evaluated using the MTT assay (**Figure 2**); the percentage of survival was calculated assuming viable untreated control cells to be 100 %. The values represent the mean of independent experiments with error bars as standard deviation (SD) (experiments were repeated 450 times each which resulted in the low values for SD). When observed under the Olympus CKX41 inverted microscope there was no evidence of morphological changes to any of the exposed L1210 progenitor cells or the L6 myoblast cells at any concentration level and with any architecture of precipitated and dialyzed PNaA. Note that concentrations levels between different samples are slightly different since the water content of each sample, as determined by TGA, was taken into account. Concentrations are expressed in $mmol \cdot L^{-1}$ of sodium acrylate units. The concentration of PNaA chains would also be relevant but it cannot be determined accurately because of the uncertainty of the molar mass values determined by SEC in the case of branched PNaA, as shown by an IUPAC working party.[45]

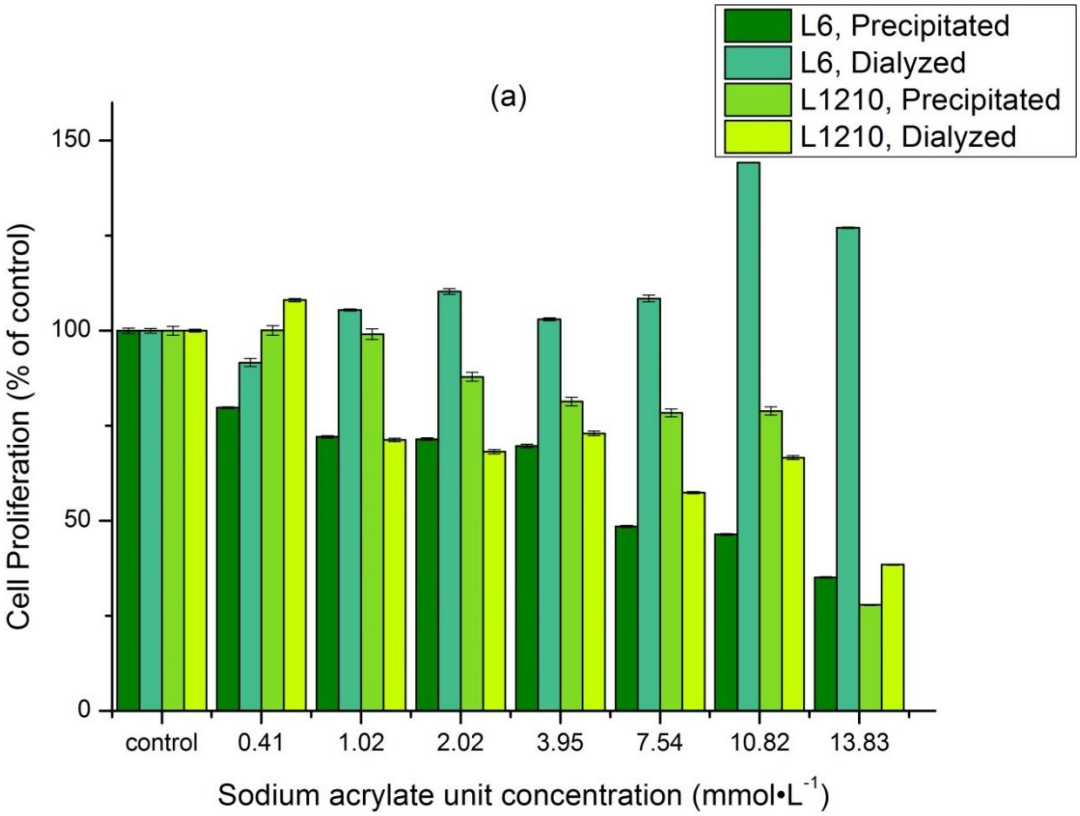
(a)
L6, Precipitated
L6, Dialyzed
L1210, Precipitated
L1210, Dialyzed
Cell Proliferation (% of control)
150
100
50
0
control
0.41
1.02
2.02
3.95
7.54
10.82
13.83
Sodium acrylate unit concentration (mmol•L-1)

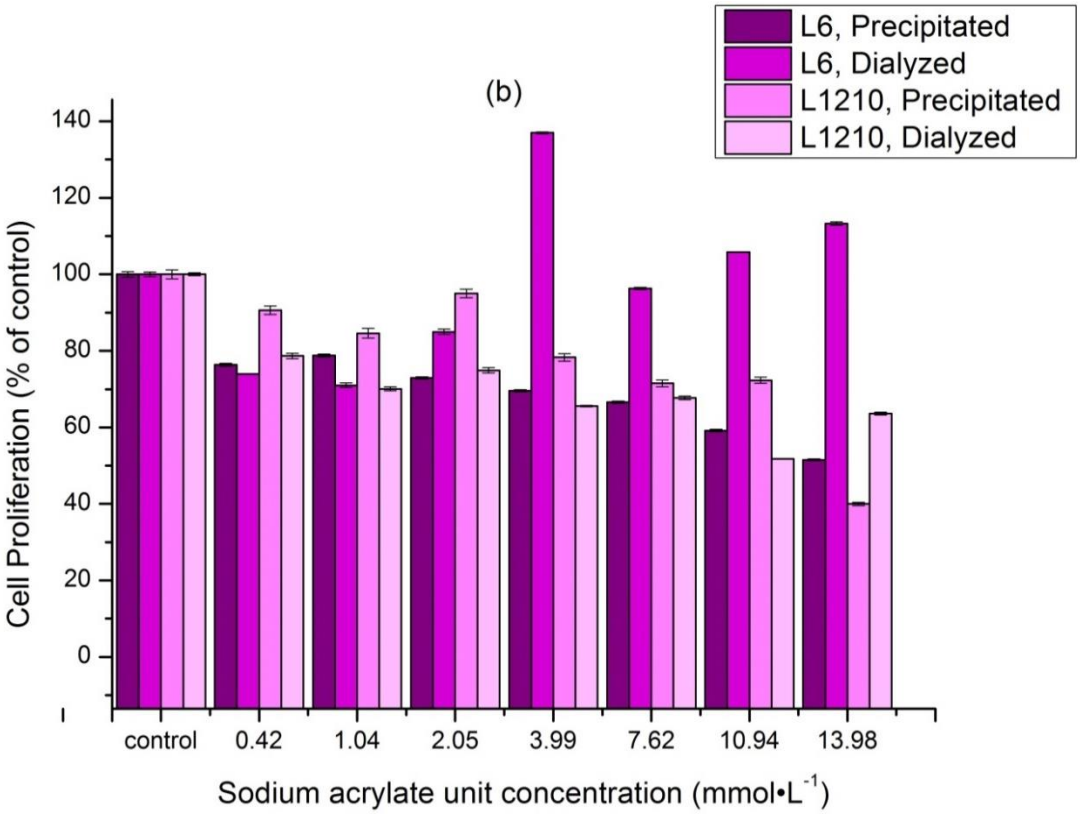
(b)
L6, Precipitated
L6, Dialyzed
L1210, Precipitated
L1210, Dialyzed
Cell Proliferation (% of control)
140
120
100
80
60
40
20
0
control
0.42
1.04
2.05
3.99
7.62
10.94
13.98
Sodium acrylate unit concentration (mmol•L-1)

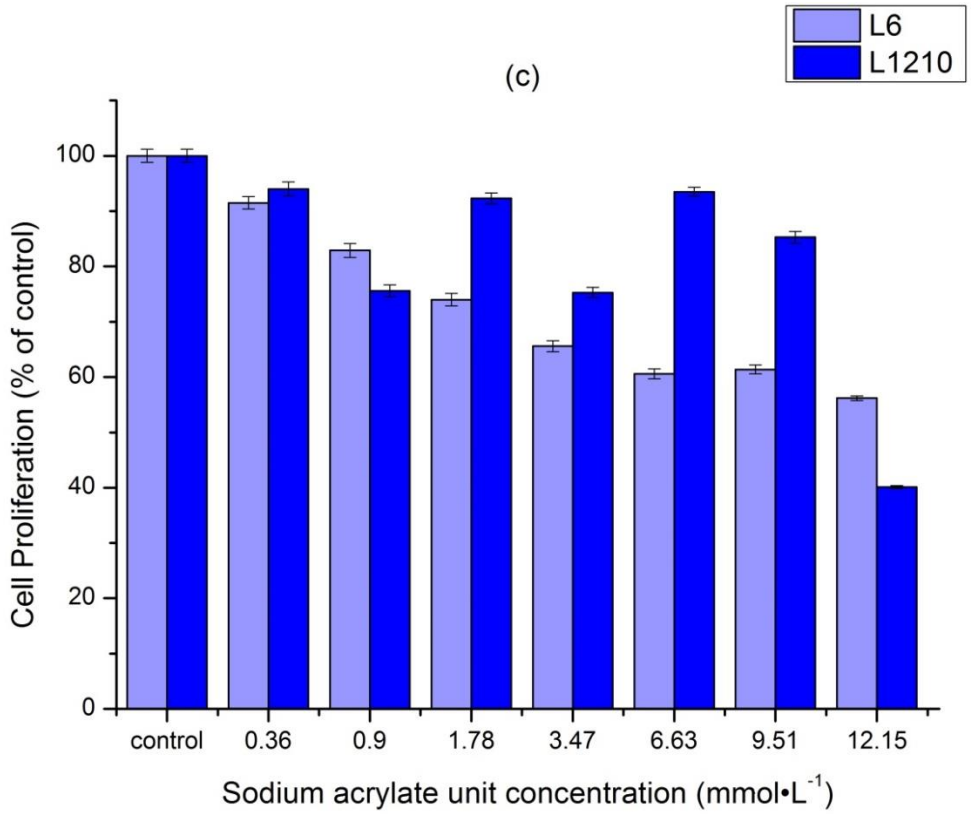

Figure 2. Graphical representations of MTT assay demonstrating the changes in cell viability of L1210 and L6 cells after a 72 h exposure to precipitated and dialyzed forms of 3-arm star (a) and hyperbranched (b) PNaA, linear (c) PNaA. Absorbance was read at 540 nm with a reference absorbance of 690 nm. The data is expressed as a percentage of cell viability compared with the untreated controls and represents the mean ± standard deviation (n=450).

After 72 h exposure both cell lines experienced the same proliferation trend with viability decreasing as the concentration of precipitated 3-arm star PNaA is gradually increased (Figure 2 a). L1210 progenitor cells suffered an acute toxic effect from precipitated 3-arm star PNaA with a dramatic decrease in percentage proliferation with the Inhibitory Concentration (IC_{50}) falling between 10.8 and 13.8 $mmol \cdot L^{-1}$ of sodium acrylate units. L6 cells appear to have a higher sensitivity to precipitated 3-arm star PNaA with their percentage

proliferation decreasing at a faster rate than that of the L1210 cell line. L6 cells do not appear to have an acute dose-responsive drop in viability as their proliferation decreases gradually as the concentration is increased. The IC_{50} occurred at 7.5 $mmol \cdot L^{-1}$ of sodium acrylate units.

L1210 and L6 cells both demonstrated an overall decrease in cell proliferation and viability as the concentration of precipitated hyperbranched PNaA was increased (Figure 2b). The L1210 cells experienced an IC_{50} between the concentration values of 10.9 and 14.0 $mmol \cdot L^{-1}$ of sodium acrylate units. L6 cells' IC_{50} occurred at 14.0 $mmol \cdot L^{-1}$ of sodium acrylate units. The toxic effect on both cell lines is acute but not as intense as the cytotoxicity experienced by cells exposed to precipitated 3-arm star PNaA.

Like precipitated 3-arm star PNaA and hyperbranched PNaA, linear PNaA also displayed an IC_{50} but it appeared to be the least cytotoxic branching architecture (Figure 2c). L1210 cells experienced their IC_{50} between 9.5 and 12.2 $mmol \cdot L^{-1}$ of sodium acrylate units. However the decrease in percentage proliferation of L1210s is not gradual as it with other architectures, showing that L1210 cells are not as sensitive to PNaA in its linear form. An IC_{50} was not determined for L6 cells, the overall proliferation decrease occurred in a gradual fashion for linear PNaA.

The residual dioxane and sodium acrylate monomer present in the precipitated 3-arm star PNaA and hyperbranched PNaA could have an effect on the results of the MTT assay; these impurities were thus removed from the samples by dialysis. L1210 cells exposed to dialyzed 3-arm star PNaA experienced an IC_{50} around 13.8 $mmol \cdot L^{-1}$ of sodium acrylate units. After exposure to dialyzed hyperbranched PNaA, an IC_{50} was only experienced in the L1210 cell line (see Figure 2 b), at a similar concentration range as to what was experienced with precipitated hyperbranched PNaA. However, an IC_{50} was not established for the L6 cell line for both dialyzed 3-arm star and hyperbranched PNaA; an increase in cell viability to rates

above controls was observed instead. In the L1210 cell line the IC_{50} of both precipitated and dialyzed 3-arm star and hyperbranched PNaA appear to occur at similar concentrations, indicating that precipitation is a sufficient purification process for this polymer to be exposed to cells as both the precipitated and dialyzed forms of PNaA behave the same as the linear PNaA which is considered to be pure.

The results seen in L6 myoblast cells exposed to dialyzed 3-arm star and hyperbranched PNaA showing viability rates above that of controls could indicate a problem with the use of the MTT assay as the cell based cytotoxicity assay for this study. As the MTT assay determines viability in relation to the mitochondrial activity of cells these results could potentially indicate that PNaA is having an effect on cellular mitochondria production, thus bringing into question the validity of these results and applicability the MTT to measure the cytotoxicity of PNaA.

It has been previously reported that some antioxidants can increase MTT reduction without having any positive effect on cell viability or proliferation.[46, 47] The fact that the increase in MTT reduction observed in L6 cells treated with dialysed 3-arm star and hyperbranched PNaA might be caused by an overstimulation of mitochondrial succinate dehydrogenases and not due to a dramatic increase in cellular proliferation. The increase in activity of mitochondrial succinate dehydrogenase would enable damaged cells to reduce MTT and increase formazan production by the same number of cells.[48] This would result in an underestimation of the potential antiproliferation effect of PNaA due to the probable increased activity of mitochondrial succinate dehydrogenase in response to PNaA treatment.

The polyester poly(3-hydroxybutyrate) (PHB) has been found to target mitochondria. It can enter cells and accumulate in the energised mitochondria and induce depolarization of the mitochondrial membrane.[49] The accumulation of PHB in cellular mitochondria suggests that

there is an active membrane transport system which allows the accumulation of PHB. The same membrane transport system that allows the accumulation of PHB might allow the accumulation of PNaA in cellular mitochondria which could affect MTT reduction.

Previous studies concluded formulations containing PNaA do not appear have a cytotoxic effect on cell proliferation and viability on a variety of cell lines, both human and from mouse.[10, 15-17] Most cells are 1-100 μm in size and can ingest particles that are smaller than 100 nm (0.1 μm). The 3-arm star, hyperbranched and linear PNaA in solution used in this study are approximately 0.6 nm (3-arm star PNaA), 0.8 nm (hyperbranched PNaA) and 1.6 nm (linear PNaA) in size (see Equation S-1 and Table S-1) implying that they could be easily absorbed into cells. The approximate size of polymers corresponds to the hydrodynamic radius calculated from the Einstein relation.[50] Formulations of PAA in previous studies have been found to be larger in size. Two formulations had approximate sizes of 100 nm [15] and 200 nm respectively [16] which are too large to be absorbed by cells. The formulations tested by [10] and [17] had approximate sizes of 10 nm which could be absorbed by cells. Therefore in these studies which have PAA formulations of a larger size it is likely that they were not directly related to the in vitro cytotoxicity of PAA macromolecules, even though these formulations might lead to the long-term release of PAA macromolecules during or after drug release. For the formulation composed of 100 nm gelatin spheres with PAA encased within the spheres [15], the cytotoxicity is not actually a measurement of PAA's cytotoxicity as little to no PAA comes into contact with cells (as it is not released from the sphere at least on the short-term). The formulation consisting of 200 nm composite microspheres is made up of 200 nm hollow microspheres of CaF_2:Ce^{3+}/Tb^{3+} held together by a PAA polymer chain [16] so even if it could be ingested by cells it is likely the concentration/amount of PAA which cells are exposed to would be negligible. For the formulation consisting of spherical silica particles

(approximately 10 nm in size) capped with a thin PAA layer [17], the concentration/amount of PAA the cells were exposed to was very small and likely insignificant for testing.

The concentrations of PNaA that were used in the MTT assay are below the critical concentration *C** (*C** is the limit between dilute and semi-dilute solutions, **Table 2**). In terms of possible formulation for chemotherapy (i.e. anticancer drug delivery) PNaA may have to be used in dilute conditions only.

Table 2. Relevant concentrations for 3-arm star, hyperbranched and linear PNaA: IC_{50} determined by the MTT assay compared to the critical concentration. All concentrations listed are in mmol·L^{-1} of sodium acrylates unit.

Architecture	**IC_{50}**		**Critical concentration *C****
	L1210 progenitor cells	**L6 myoblast cells**	
Precipitated Hyperbranched PNaA	13.98	13.98	740
Dialyzed hyperbranched PNaA	- [a)]	- [a)]	740
Precipitated 3-arm star PNaA	10.82 to 13.83	7.54	222
Dialyzed 3-arm star PNaA	13.83	- [a)]	222
Linear PNaA	12.15	>12.15	553

[a)] Value not attained

The branched PNaAs have SG1 as an end group. According to industry manufacturer Arkema SG1 has a good toxicological profile.[51] A purity of 96 % free SG1 did not affect cell viability of the NIH/3T3 (embryonic murine fibroblast) cells and J774.A1 (murine macrophage) cells at concentrations of 0.34 mmol·L^{-1} and 1.02 mmol·L^{-1}.[52] In the PNaA

architectures used in this study there is only one group of SG1 for hundreds of sodium acrylate units. For example in the concentration of precipitated and dialyzed forms of 3-arm star PNaA that caused an IC_{50} in L1210 progenitor cells, there is approximately 0.118 to 0.157 mmol·L^{-1} and approximately 0.784 mmol·L^{-1} of SG1 present at the L6 myoblast IC_{50}. At the concentration where precipitated and dialyzed hyperbranched PNaA cause an IC_{50} in both L1210 progenitor cells and L6 myoblast cells there is approximately 0.108 mmol·L^{-1} of SG1 present. It is therefore highly unlikely that the presence of SG1 is the cause of the cytotoxicity experienced in cells exposed to PNaA.

3.4. PNaA – Lipid Bilayer

Spectral analysis of lipid components stained with Nile Red (2.5 μg·mL^{-1}) in L6 myoblast cells treated with precipitated samples was carried out for 3-arm star PNaA, hyperbranched PNaA and linear PNaA at concentrations of 3.19, 3.22 and 2.80 mmol·L^{-1} of acrylic acid units respectively for 24 h in a culture environment containing 10 % v/v serum. Only precipitated samples were used in these experiments because it is the golden standard of polymer purification and requires less time and only L6 cells were used for practicality because they are an adherent cell line thus allowing for easier acquisition of data. There was a slight blue shift in the emission spectra of lipid components (data not shown), i.e. shift to a lower wavelength, of lipid droplets (cholesterols and triglycerides) by 10 nm from approximately 596 nm in untreated control cells to 586 nm in PNaA treated cells. Phospholipids also experienced a blue shift from 633 nm in control cells to 622 nm in treated cells.

The concentration of Nile Red to stain L6 myoblast cells had a concentration-dependent effect on the differential staining of lipid components. Using a lower Nile Red concentration

(0.5 $\mu g \cdot mL^{-1}$) did not provide a sufficient level of fluorescence for imaging. Increasing the laser power to increase fluorescence is not desired as it induces rapid photobleaching, and increasing the smart gain increased the level of background fluorescence. While opening the pinhole did result in an increase in fluorescence, it was at the expense of resolution. Staining L6 cells with a higher concentration of Nile Red resulted in the staining of phospholipids and no staining of cholesterols and triglycerides. The concentration effect of Nile Red is supported by a report of excitation and emission maxima of Nile Red dependent on the dye's concentration.[53] Nile Red at lower concentrations exhibits an emission maximum at a shorter wavelength than at higher concentrations. This emphasizes the importance of using a single concentration of Nile Red throughout all experimental work to limit variation between data sets.

The effect of precipitated samples of 3-arm star PNaA, hyperbranched PNaA and linear PNaA in the shift of the emission maximum was found to be consistent with an investigation of the effect of PAA on the fluorescence properties of tryptophan residues in the protein from bovine serum albumin (BSA).[42] PAA reduced the fluorescence of tryptophan and shifted its emission maximum towards the blue region. Increasing the concentration of PAA in BSA-PAA mixtures resulted in a decrease in tryptophan fluorescence intensity, this effect was more pronounced as the solutions pH was further decreased. PAA was also found to induce some blue shift in the emission maximum of tryptophan residues which were more pronounced at higher PAA concentrations and lower solution pHs of the BSA-PAA mixtures. At pH 7, the emission maximum of the BSA-PAA mixtures at the maximal ratio of PAA to BSA was at 335 nm but at pH 4, the BSA-PAA mixtures at the same ratio showed a sufficiently larger blue shift to 320 nm.

L6 myoblast cells exposed to a concentration of 3.2 mmol·L^{-1} of sodium acrylate units of precipitated 3-arm star PNaA for 1 h in 0 % serum and 24 h in 2 % serum displayed an effect on cellular lipid distribution with the presence of orange droplets being noted. No visual effects were observed to cells incubated in precipitated 3-arm star PNaA for 1 h in 2 %, 5 % and 10 % serum and 24 h in 5 % and 10 % serum.

Hyperbranched PNaA at a concentration of 3.2 mmol·L^{-1} of sodium acrylate units had a similar trend to the lipid distribution observed in 3-arm star PNaA exposure. Cells exposed to precipitated hyperbranched PNaA for 1 h in 0 % serum and 24 h in 2 % serum had visible orange droplets (**Figure 3**). Cells incubated in hyperbranched PNaA for 1 h in 2 %, 5 % and 10 % serum and 24 h in 5 % and 10 % serum displayed green-yellow droplets.

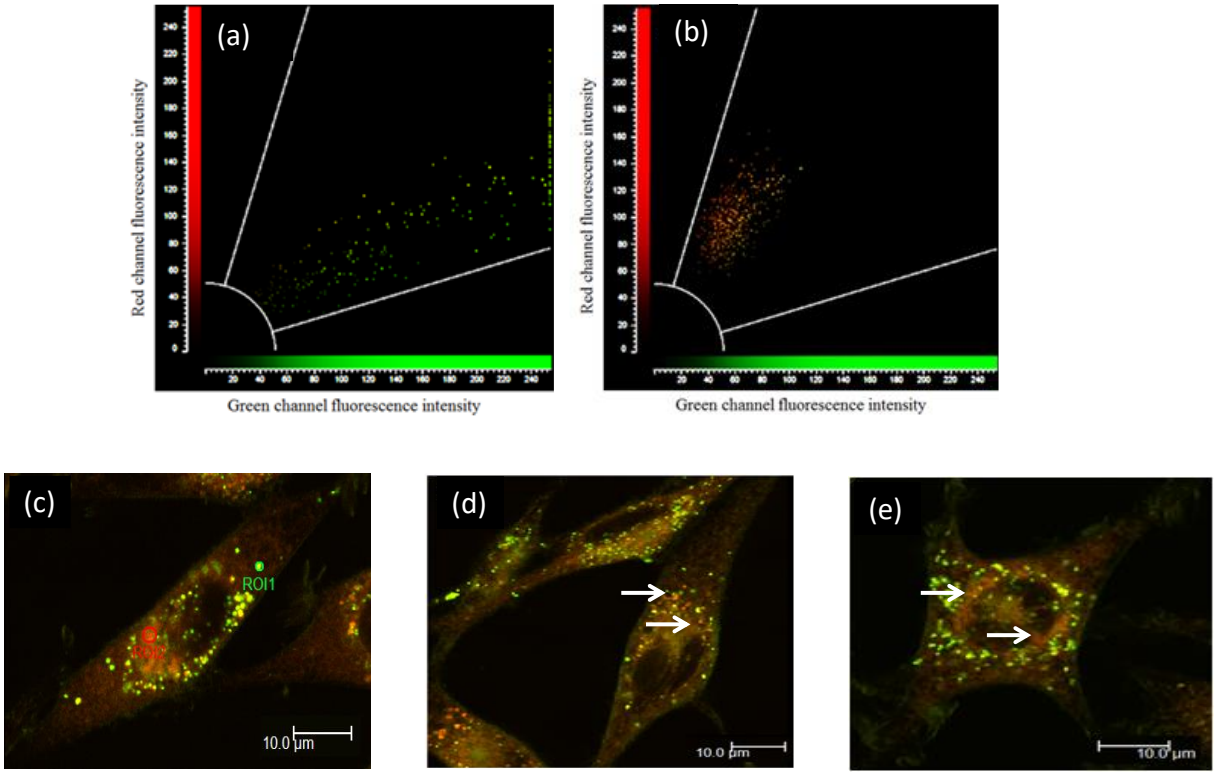

Figure 3. Co-localization of L6 myoblast cells stained with Nile Red (2.5 µg·mL^{-1}). (a) and (b) show the degree of co-localization in green and red channels for a selected region of interest (ROI). (c) displays the ROI1 (green) corresponding with (a) which surrounds an area of intense green staining and ROI2 (red) which corresponds to (b) which surrounds an area of

diffuse red staining. (d) is a control L6 myoblast cell after a 24 h incubation with 5 % serum, (e) is an L6 cell after a 24 h exposure to precipitated hyperbranched PNaA with 5 % serum. White arrows indicated the merging of cellular lipids.

L6 myoblast cells incubated in precipitated linear PNaA at a concentration of 2.8 mmol·L^{-1} of sodium acrylate units for 1 h in 0 % serum, 24 h in 2 % serum and 24 h in 5 % serum was found to have an effect on lipid distribution. The presence of orange lipid droplets was more abundant in cells exposed to linear PNaA for 24 h in 2 % serum than other tested time courses and serum concentrations which had few orange droplets. L6 cells exposed to linear PNaA (in the same concentration) for 1 h with 2 %, 5 % and 10 % serum and 24 h with 10 % serum did not appear to have any changes in lipid regions within the cell.

The changes in lipid distribution as demonstrated by the observation of orange lipid droplets after exposure to PNaA for 1 h in 0 % serum and 24 h in 2 % serum appear to be caused by a possible merger of cellular lipids. Co-localization analysis in the regions of intense orange staining (data not shown) plots most of the pixels along the red channel with some falling towards the center boundary of the co-localization scatter plot (Figure 3 a, b and c). This indicates that the orange lipid droplets exhibit most fluorescence from the red channel with some degree of co-localization suggesting the merge of lipid droplets (possibly cholesterols and triglycerides) with phospholipids. However it should be noted that a similar merge of cellular lipids was observed in control groups subjected to the same conditions (Figure 3 d and e), therefore the merge may be a result of the serum deprivation and not directly due to the presence of PNaA. Nile Red has been previously shown to intensely fluoresce when combined with serum lipoproteins, especially for very low density lipoproteins which can cause a blue spectral shift.[42] Starving L6 cells of serum appears to have resulted in a reduced

concentration of serum lipoproteins and resulting in a lower spectral blue shift and hence the orange staining of lipid droplets.

4. Conclusions

PNaA interacted with serum proteins as demonstrated by capillary zone electrophoresis and this was observed for linear, 3-arm star and hyperbranched structures.

In the concentrations used in the study precipitated and dialyzed PNaA was found to have a dose-dependent cytotoxicity on L1210 mammalian cells tested. Linear PNaA was determined to be the least cytotoxic architecture, followed by precipitated hyperbranched PNaA. Precipitated 3-arm star PNaA was found to be the most cytotoxic architecture of PNaA in its precipitated form. Differences in the branching architecture of PNaAs did not change the cytotoxicity greatly as expected. Nitroxide mediated polymerization (NMP) of acrylic acid followed by precipitation lead to detectable amount of residual solvent (1,4-dioxane) and monomer in the PNaA as shown by ^{1}H NMR. The residual impurities are removed, at least at 95 %, by dialysis. After dialysis, both the 3-arm star and hyperbranched PNaA architectures caused an IC_{50} on the L1210 progenitor cells at similar concentration levels as the precipitated form. This indicates that in its precipitated form PNaA has a cytotoxicity that belongs to the polymer and not to the residual solvent and monomer that result from synthesis. Precipitation is a sufficient purification process on its own for PNaA and no additional or secondary purification steps were required. However, the dramatic increase in L6 myoblast cells viability seen in dialyzed 3-arm star and hyperbranched PNaA experiments indicates that the MTT may not be a suitable cell based cytotoxicity assay for this study.

While exposure to PNaA in different serum concentrations suggests that PNaA in the current architectures has an effect on cellular lipid distribution, the change in lipid distribution and merge of cellular lipids are more likely the result of serum starvation and not of PNaA exposure.

To follow on from this work a different cell based viability assay will be used, such as dead-cell protease, DNA or a apoptosis/neurosis based assays like the CytoTox-Glo™ Cytotoxicity Assay, the PicoGreen® assay or a Apoptotic and Necrotic Detection kits to determine the cytotoxicity of PNaA [54-56]. Further quantitative work on PNaA serum interactions via CE will be conducted. A fluorophore will also be attached to PNaA to better visualize it via confocal fluorescent microscopy and determine if PNaA is actually entering cells and if so where it is localizing.

Supporting Information

Supporting Information is available from the Wiley Online Library or from the author

Acknowledgements: thanks to Dr Simon Hager, Dr Richard Wuhrer and the Advanced Materials Characterisation Facility (AMCF) at the University of Western Sydney for TGA measurements, and to Prof. Hervé Cottet (Montpellier, France), Prof. Jens Coorssen, Danielle Taylor and Adam Sutton (UWS) for discussions.

Received: Month XX, XXXX; Revised: Month XX, XXXX; Published online: ; DOI: 10.1002/mabi.201500153

Keywords: poly(acrylic acid) / poly(sodium acrylate), cytotoxicity, MTT assay, cell, capillary electrophoresis

[1] S. R. Abulateefeh, S. G. Spain, J. W. Aylott, W. C. Chan, M. C. Garnett, C. Alexander, *Macromol. Biosci.* **2011**, *11*, 1722.

[2] M. Callari, J. R. Aldrich-Wright, P. L. de Souza, M. H. Stenzel, *Progr. Polym. Sci.* **2014**, *39*, 1614.

[3] A. K. Patri, I. J. Majoros, J. R. Baker, *Curr. Opin. Chem. Biol.* **2002**, *6*, 466.

[4] A. Kumar, A. Srivastava, I. Y. Galaev, B. Mattiasson, *Prog. Polym. Sci.* **2007**, *32*, 1205.

[5] D. Schmaljohann, *Adv. Drug Deliv. Rev.* **2006**, *58*, 1655.

[6] I. F. Tannock, D. Rotin, *Cancer Res.* **1989**, *49*, 4373.

[7] Y. Mochida, H. Cabral, Y. Miura, F. Albertini, S. Fukushima, K. Osada, N. Nishiyama, K. Kataoka, *ACS Nano* **2014**, *8*, 6724.

[8] N. Nishiyama, M. Yokoyama, T. Aoyagi, T. Okano, Y. Sakurai, K. Kataoka, *Langmuir* **1999**, *15*, 377.

[9] L. Y. Qiu, Y. H. Bae, *Pharm. Res.* **2006**, *23*, 1.

[10] A. Kowalczuk, E. Stoyanova, V. Mitova, P. Shestakova, G. Momekov, D. Momekova, N. Koseva, *Int. J. Pharm.* **2011**, *404*, 220.

[11] F. A. Plamper, H. Becker, M. Lanzendorfer, M. Patel, A. Wittemann, M. Ballauff, A. H. E. Muller, *Macromol. Chem. Phys.* **2005**, *206*, 1813.

[12] B. J. Boyd, *Exp. Opin. Drug Deliv.* **2008**, *5*, 69.

[13] O. E. Philippova, D. Hourdet, R. Audebert, A. R. Khokhlov, *Macromolecules* **1997**, *30*, 8278.

[14] A. R. Maniego, D. Ang, Y. Guillaneuf, C. Lefay, D. Gigmes, J. R. Aldrich-Wright, M. Gaborieau, P. Castignolles, *Anal. Bioanal. Chem.* **2013**, *405*, 9009.

[15] D. Ding, Z. Zhu, Q. Liu, J. Wang, Y. Hu, X. Jiang, B. Liu, *Eur. J. Pharma. Biopharma.* **2011**, *79*, 142.

[16] Y. L. Dai, C. M. Zhang, Z. Y. Cheng, P. A. Ma, C. X. Li, X. J. Kang, D. M. Yang, J. Lin, *Biomaterials* **2012**, *33*, 2583.

[17] Q. Wang, Y. P. Bao, X. H. Zhang, P. R. Coxon, U. A. Jayasooriya, Y. M. Chao, *Adv. Healthc. Mater.* **2012**, *1*, 189.

[18] A. van Tonder, A. M. Joubert, A. D. Cromarty, *BMC Res. Notes* **2015**, *8*, 47.

[19] A. Y. Shmykov, V. N. Filippov, L. S. Foteeva, B. K. Keppler, A. R. Timerbaev, *Anal. Biochem.* **2008**, *379*, 216.

[20] A. R. Timerbaev, B. K. Keppler, *Anal. Biochem.* **2007**, *369*, 1.

[21] P. Hong, S. Koza, E. S. P. Bouvier, *J. Liq. Chromatogr. Rel. Technol.* **2012**, *35*, 2923.

[22] J. J. Thevarajah, M. Gaborieau, P. Castignolles, *Adv. Chem.* **2014**, *2014*, Article ID 798503.

[23] J. C. Kraak, S. Busch, H. Poppe, *J. Chromatogr. A* **1992**, *608*, 257.

[24] M. Kanoatov, L. T. Cherney, S. N. Krylov, *Anal. Chem.* **2014**, *86*, 1298.

[25] M. Berezovski, S. N. Krylov, *J. Am. Chem. Soc.* **2002**, *124*, 13674.

[26] A. P. Drabovich, M. Berezovski, V. Okhonin, S. N. Krylov, *Anal. Chem.* **2006**, *78*, 3171.

[27] L. T. Cherney, M. Kanoatov, S. N. Krylov, *Anal. Chem.* **2011**, *83*, 8617.

[28] S. M. Krylova, P. M. Dove, M. Kanoatov, S. N. Krylov, *Anal. Chem.* **2011**, *83*, 7582.

[29] J. Bao, S. M. Krylova, L. T. Cherney, R. L. Hale, S. L. Belyanskaya, C. H. Chiu, C. C. Arico-Muendel, S. N. Krylov, *Anal. Chem.* **2015**, *87*, 2474.

[30] M. Kanoatov, V. A. Galievsky, S. M. Krylova, L. T. Cherney, H. K. Jankowski, S. N. Krylov, *Anal. Chem.* **2015**, *87*, 3099.

[31] G. Diaz, M. Melis, B. Batetta, F. Angius, A. M. Falchi, *Micron* **2008**, *39*, 819.

[32] H. E. Gottlieb, V. Kotlyar, A. Nudelman, *J. Org. Chem.* **1997**, *62*, 7512.

[33] J. Chamieh, M. Martin, H. Cottet, *Anal. Chem.* **2015**, *87*, 1050.

[34] C. Gartner, B. L. Lopez, L. Sierra, R. Graf, H. W. Spiess, M. Gaborieau, *Biomacromolecules* **2011**, *12*, 1380.

[35] S. Schmitz, A. C. Dona, P. Castignolles, R. G. Gilbert, M. Gaborieau, *Macromol. Biosci.* **2009**, *9*, 506.

[36] T. Caykara, O. Guven, *J. Appl. Polym. Sci.* **1998**, *70*, 891.

[37] P. Castignolles, M. Gaborieau, E. F. Hilder, E. Sprong, C. J. Ferguson, R. G. Gilbert, *Macromol. Rapid Commun.* **2006**, *27*, 42.

[38] M. C. Breadmore, C. de Griend, R. E. Majors, *LC GC N. Am.* **2014**, *32*, 174.

[39] S. S. Aleksenko, A. Y. Shmykov, S. Oszwaldowski, A. R. Timerbaev, *Metallomics* **2012**, *4*, 1141.

[40] L. T. Cherney, S. N. Krylov, *Analyst* **2015**, *140*, 2797.

[41] A. P. Petrov, L. T. Cherney, B. Dodgson, V. Okhonin, S. N. Krylov, *J. Am. Chem. Soc.* **2011**, *133*, 12486.

[42] Y. Budama Battal, M. Topuzogullari, Z. Mustafaeva, *J. Fluoresc.* **2009**, *in press*, DOI 10.1007/s10895.

[43] N. Akkilic, Z. Mustafaeva, M. Mustafaev, *J. Appl. Polym. Sci.* **2007**, *105*, 3108.

[44] M. Abdullah, J. A. Crowell, L. L. Tres, A. L. Kierszenbaum, *J. Cell Physiol.* **1986**, *127*, 463.

[45] I. Lacik, M. Stach, P. Kasak, V. Semak, L. Uhelska, A. Chovancova, G. Reinhold, P. Kilz, G. Delaittre, B. Charleux, I. Chaduc, F. D'Agosto, M. Lansalot, M. Gaborieau, P. Castignolles, R. G. Gilbert, Z. Szablan, C. Barner-Kowollik, P. Hesse, M. Buback, *Macromol. Chem. Phys.* **2015**, *216*, 23.

[46] J. T. Sims, R. Plattner, *Cancer Chemother. Pharmacol.* **2009**, *64*, 629.

[47] E. Maioli, C. Torricelli, V. Fortino, F. Carlucci, V. Tommassini, A. Pacini, *Biol. Proced. Online* **2009**, *11*, 227.

[48] P. W. Wang, S. M. Henning, D. Heber, *PLoS One* **2010**, *5*.

[49] P. A. Elustondo, P. R. Angelova, M. Kawalec, M. Michalak, P. Kurcok, A. Y. Abramov, E. V. Pavlov, *PLoS One* **2013**, *8*.

[50] P. Castignolles, M. Gaborieau, *J. Sep. Sci.* **2010**, *33*, 3564.

[51] Arkema, "BlocBuilder Controller Technology For Block Copolymers", **2006**, www.arkema-inc.com/literature/pdf/770.pdf.

[52] M. Chenal, S. Mura, C. Marchal, D. Gigmes, B. Charleux, E. Fattal, P. Couvreur, J. Nicolas, *Macromolecules* **2010**, *43*, 9291.

[53] P. Greenspan, S. D. Fowler, *J. Lipid Res.* **1985**, *26*, 781.

[54] M.-H. Cho, A. Niles, R. Huang, J. Inglese, C. P. Austin, T. Riss, M. Xia, *Toxicol. In Vitro* **2008**, *22*, 1099.

[55] Life Technologies™, Quant-iT™ PicoGreen® dsDNA Assay Kit, https://www.lifetechnologies.com/order/catalog/product/P7589, accessed: April, 2015.

[56] PromoKine, Apoptotic & Necrotic Cell Differentiation, http://www.promokine.info/products/apoptosis/apoptotic-necrotic-cell-detection-kits/, accessed: April, 2015.

Table of Contents

The cytotoxicity and intracellular effects of poly(acrylic acid) / poly(sodium acrylate) (PNaA) are investigated. This pH-responsive polymer has potential in anticancer drug delivery. Capillary electrophoresis demonstrates interactions of PNaA with serum proteins. The MTT assay is used to assess the cytotoxicity of PNaA with different branching architectures for L1210 progenitor leukemia cells and L6 myoblast cells.

E. G. Whitty, A. R. Maniego, S. A. Bentwitch, Y. Guillaneuf, M. R. Jones, M. Gaborieau*, P. Castignolles

Cellular Response to Linear and Branched Poly(acrylic acid)

ToC figure

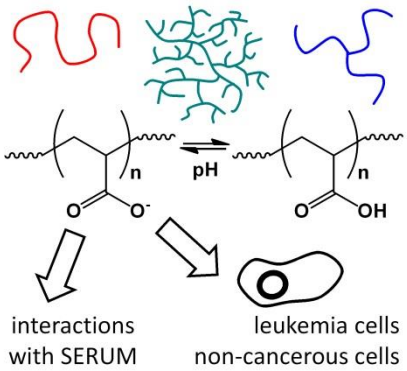

Supporting Information

for *Macromol. Biosci.*, DOI: 10.1002/mabi.201500153

Cellular response to linear and branched poly(acrylic acid)

Elizabeth G. Whitty, Alison R. Maniego, Sharon A. Bentwitch, Yohann Guillaneuf, Mark R. Jones, Marianne Gaborieau*, Patrice Castignolles

Cytotoxicity Method

In metabolically active cells (viable cells) mitochondrial dehydrogenase enzymes convert 3-[4,5-dimethylthiazol-2-yl)]-2,5-diphenyl-tetrazolium bromide (MTT or tetrazolium salt) into purple formazan crystals, which are dissolved with dimethyl sulfoxide (DMSO) and the optical density is measured via a spectrophotometer.[1] Since mitochondrial dehydrogenase enzymes are only active in living cells the measured optical density is expected to be directly proportional to the number of live cells tested.[2]

In MTT methodology both L6 adherent cells and L1210 non-adherent cells had 170 µL of medium and residual architectures removed. 170 µL was established as being an acceptable amount to be removed without affecting MTT results for non-adherent cells. As non-adherent cells do not adhere to the bottom of the well they have the potential to disperse throughout the medium. However due to gravitational forces L1210 cells have been observed to sink to the bottom of wells and remain there if not agitated. To determine an appropriate amount of medium that could be removed from the well without affecting the MTT results varying amounts of medium was removed from wells and observed under an inverted light microscope to determine the presence of any cells. As cells had minimal movement over the experimental period cells had remained at the bottom of the well and the removed 170 µL of medium did not contain cells and thus did not affect MTT results for L1210 non-adherent cells. PNaA samples were introduced into the culture medium via pipetting directly into media and the plates were then moved to temperature controlled incubator and left undisturbed for the experimental time course.

Assessment of PAA Dialysis

A diluted conventional PAA (Sigma-Aldrich) was injected in CE (see below) at 0.00008 $mg \cdot mL^{-1}$. Equivalent amount in the dialysate was found to be a 0.03 mg total loss from 45 mg originally in dialysis membrane. The electrophoretic mobility of the traces detected on Figure S1 in the dialysate correspond to oligo(acrylic acid).[3] Figure S2 show the ^{1}H NMR spectra of the PAA before and after dialysis.

CE Method

The CE method is the same as in the main text except for what follows. A high sensitivity capillary of 50 μm i.d. with a 62 or 60.2 cm total length and a 53.5 or 51.7 cm effective length to the detector was used. The capillary was preconditioned with a 5 min flush with 110 mM sodium borate phosphate buffer at pH 9.2. The acquisition time was 20 min. A diode array detector was used at a wavelength of 195 nm with a 10 nm bandwith. Milli-Q water was injected with a pressure of 30 mbar for 30 s, sample was injected with pressure of 30 mbar for 135 s. The voltage for all separations was 30 kV at 25 °C.

CE Results

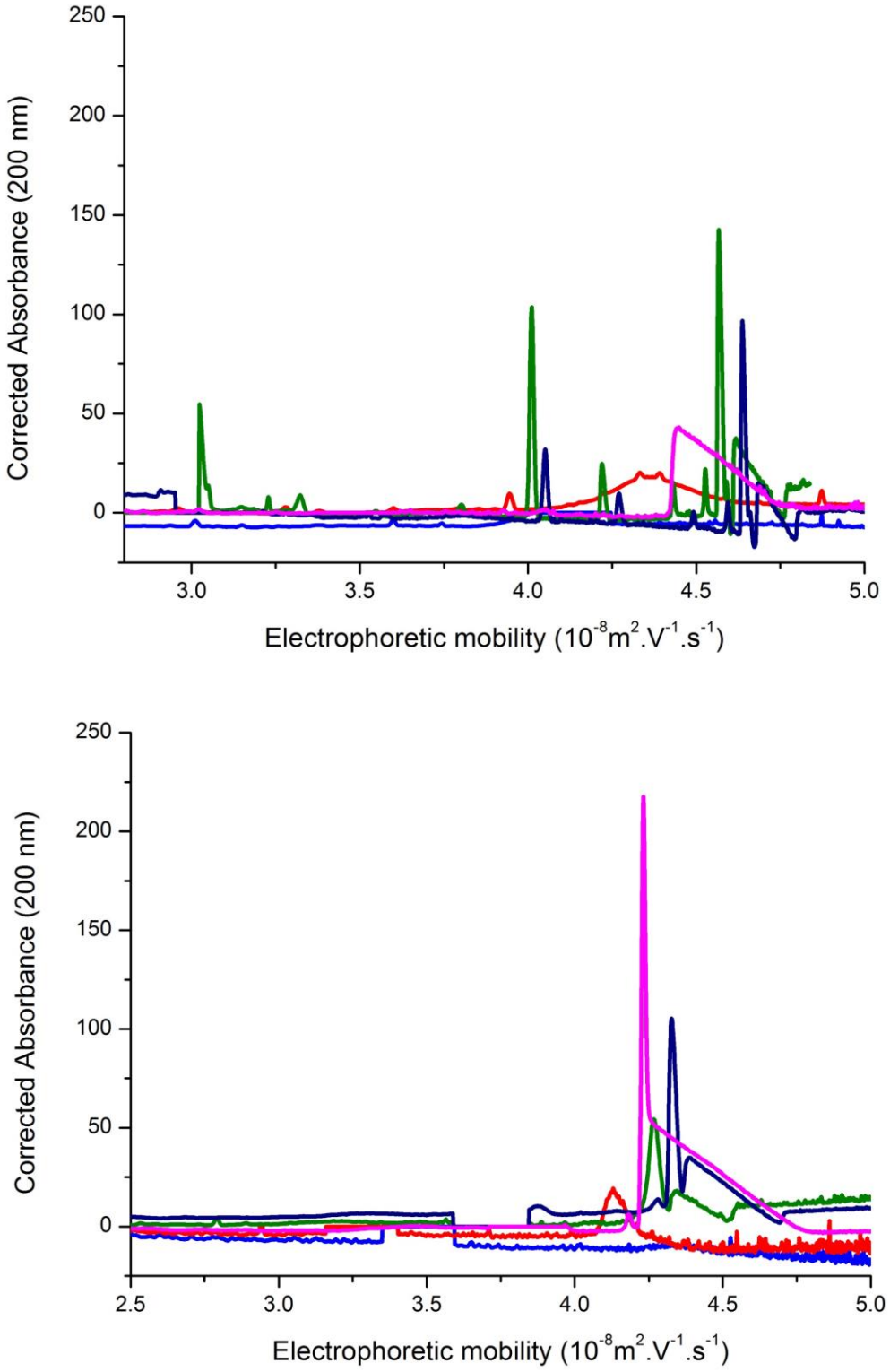

*Figure S1***.** CE of dialysate of 3-arm star PAA (top) and hyperbranched PAA (bottom). Dialysis series 1 (red), dialysis series 2 (blue), membrane rinse with NaOH immediately following completion of dialysis series (olive), membrane rinse after soaking in NaOH for 1 h (navy) and membrane rinse after soaking in NaOH overnight (magenta).

NMR Results

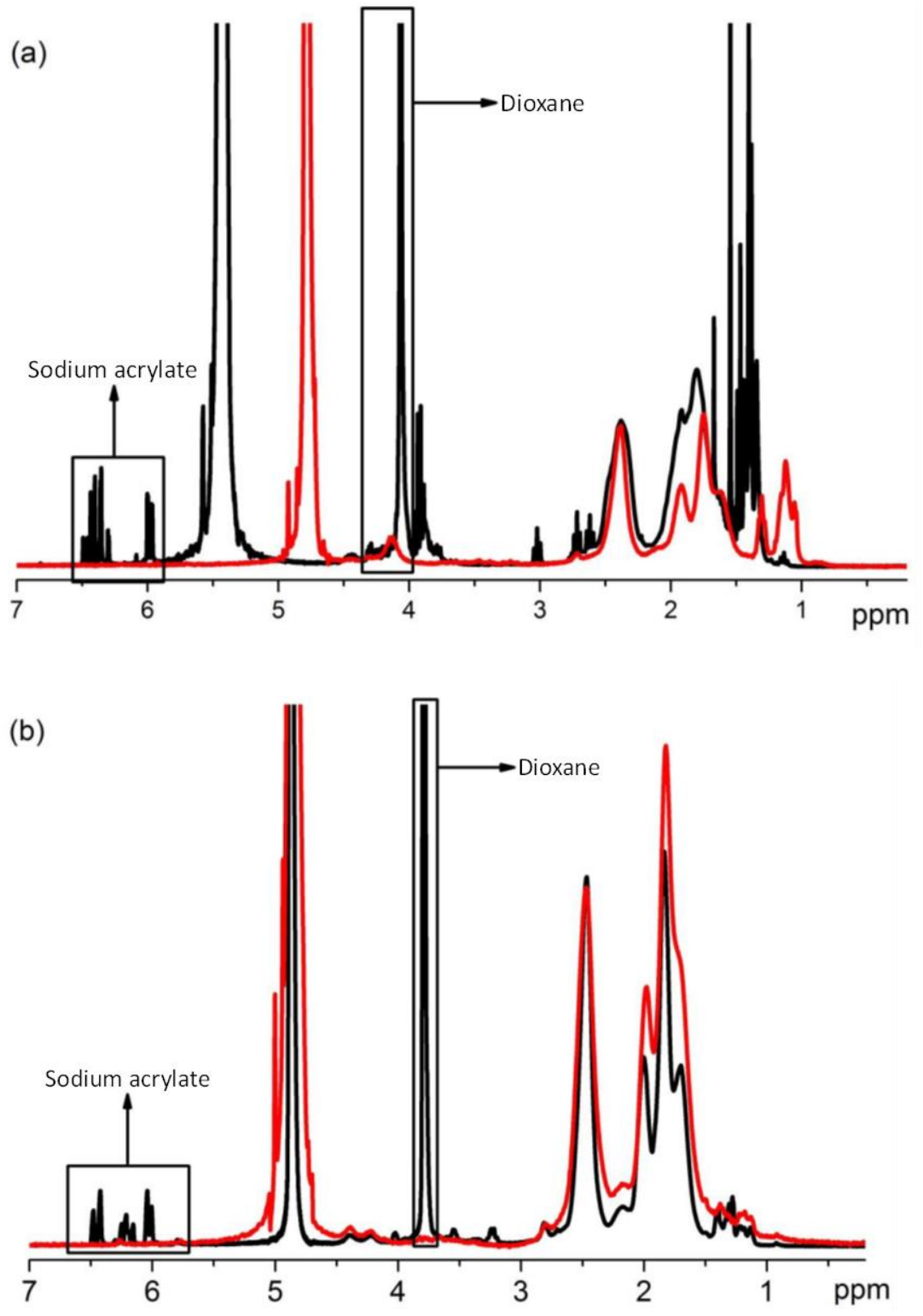

*Figure S2***.** ^{1}H NMR spectra of the precipitated (black) and dialyzed (red) 3-arm star (a) and hyperbranched (b) PNaAs in D_2O.

No residual 1,4-dioxane or sodium acrylate monomer was observed in linear PNaA. The vinylic signals of sodium acrylate residual monomer and the signals of 1,4-dioxane were observed for the precipitated polymers at 6 – 6.5 ppm and at 3.7 - 4 ppm respectively. Note that the routine conditions used to record the ^{1}H NMR spectra, in particular the short repetition delay between scans, prevented the quantification of the detected impurities. The residual sodium acrylate signals were absent after the dialysis process. The 1,4-dioxane signal for the hyperbranched PNaA were also not observed after dialysis while a negligible 1,4-dioxane signal (~ 5 % of the original residual 1,4-dioxane peak) was detected after the dialysis of the 3-arm star PNaA.

Moisture Content by TGA

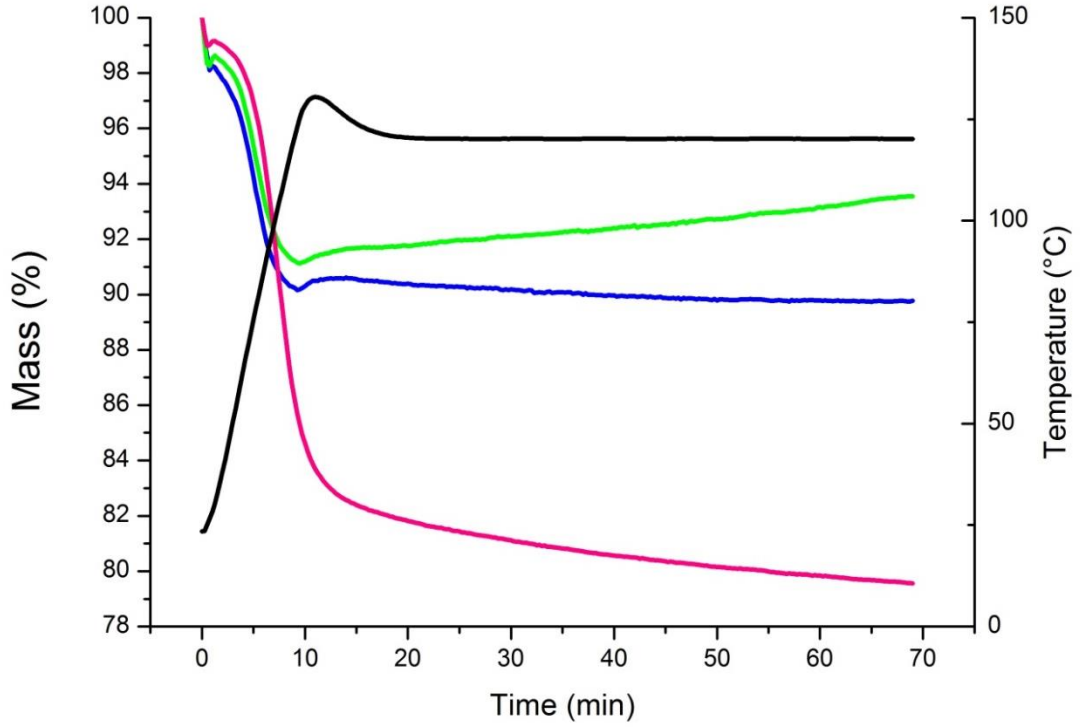

Figure S3. TGA thermogram of the linear (pink), dialyzed 3-arm star (blue) and hyperbanched (green) PNaA. Temperature over time is represented via the black line.

Capillary Electrophoresis to Assess PNaA – Proteins Interactions

Materials

50 µm internal diameter fused silica capillaries coated with a poly(ethylene oxide) coating (µSiL-WAX capillary, Agilent Technologies) with a total length of 54 cm, effective length of 45.5 cm, or coated with fluorinated polymer (µSiL-FC capillary, Agilent Technologies) with a total length of 62.2 cm, effective length of 53.7 cm, were used.

A 50 mL stock sodium phosphate buffer at a concentration of 500 mM was prepared by dissolving 3.549 g of sodium phosphate dibasic anhydrous (Sigma) in 40 mL Milli-Q water and titrating it with 14.5 mM of orthophosphoric acid (Fisons Pharmaceutical) to pH 7.4. The stock buffer solution was topped up to 50 mL with Milli-Q water and stored at 4°C. 50 mL of sodium phosphate buffer at 10 mM (PB10) was prepared by diluting 1 mL of stock sodium phosphate buffer solution with 49 mL Milli-Q water and stored at 4 °C.

Methods

The preconditioning of µSiL-WAX capillary consisted of a 5 min flush with absolute ethanol, a 5 min flush with Milli-Q water, a 2 min flush with 10mM orthophosphoric acid, a 5 min flush with Milli-Q water and a final 10 min flush with phosphate buffer (PB10 at pH 7.4). The samples were hydrodynamically injected at 30 mbar for 10 s and subjected to a voltage of 30 kV at 37 °C. After the final separation post-conditioning consisted of flushing for 2 min with 10 mM orthophosphoric acid, for 20 min with Milli-Q water, for 5 min with absolute ethanol and for 10 min with air to dry the capillary. Preconditioning was performed before every injection to clean the capillary between consecutive separations.

Results With a BGE in Physiological Conditions

The electrostatic repulsion experienced between the partially negative PAA at pH 7.4 and the negative charge of uncoated capillary surfaces is not strong and resulted in PAA interacting and adsorbing onto the capillary wall.

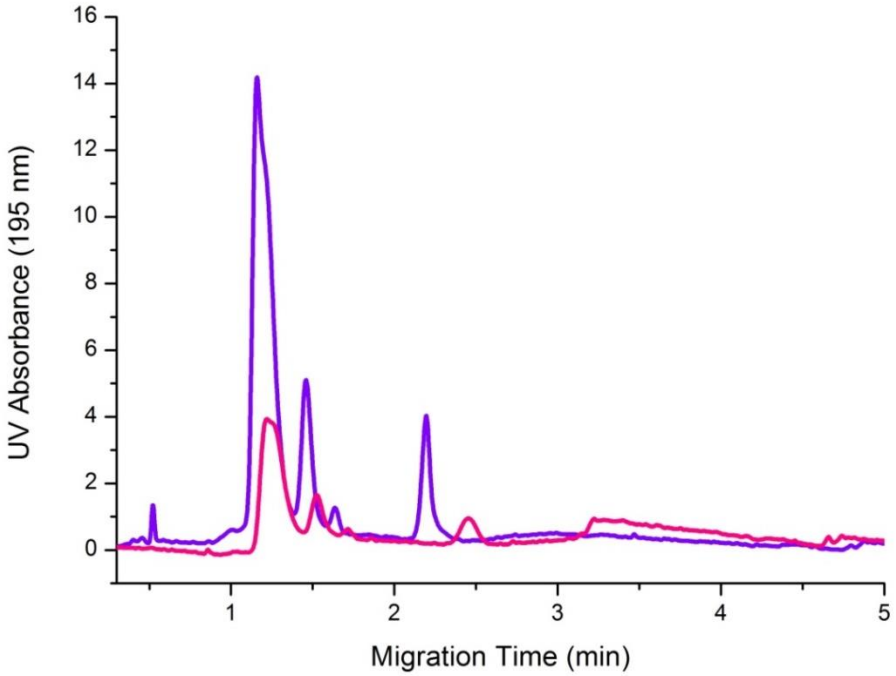

Figure S4. Capillary electrophoresis electropherograms showing limited repeatability of the separation of an oligoacrylate standard (AA4 [29]) in sodium phosphate buffer (50 mM) at pH 7.4 in μSiL-FC capillary. The first run is represented by the purple line and the pink line represents the second run.

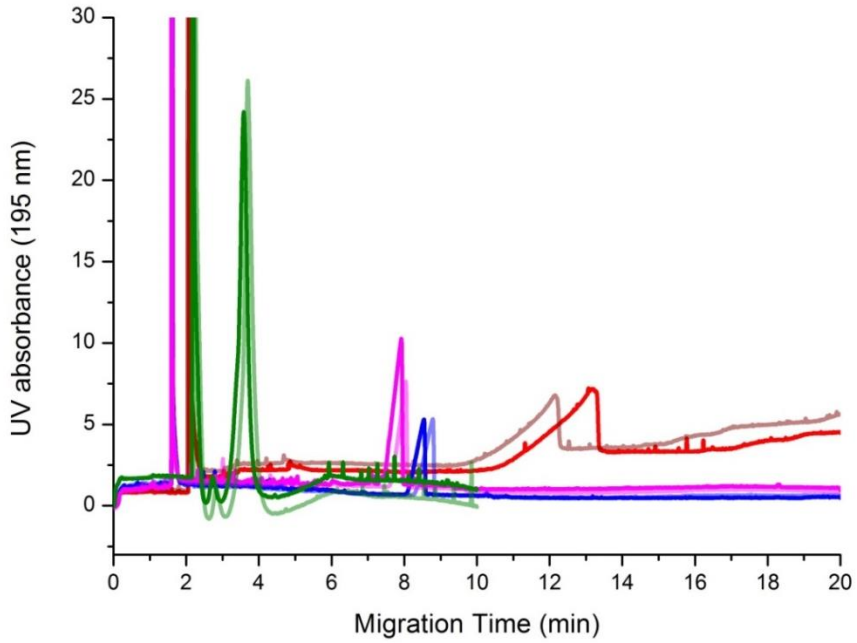

Figure S5. Repeatability of run-to-run separations of linear PNaA (red and wine), 3-arm star PNaA (light and dark blue), hyperbranched PNaA (light and dark pink) and 10 % foetal bovine serum (light and dark green) in sodium phosphate buffer (10 mM) at pH 7.4 and 37 °C in a μSiL-WAX capillary.

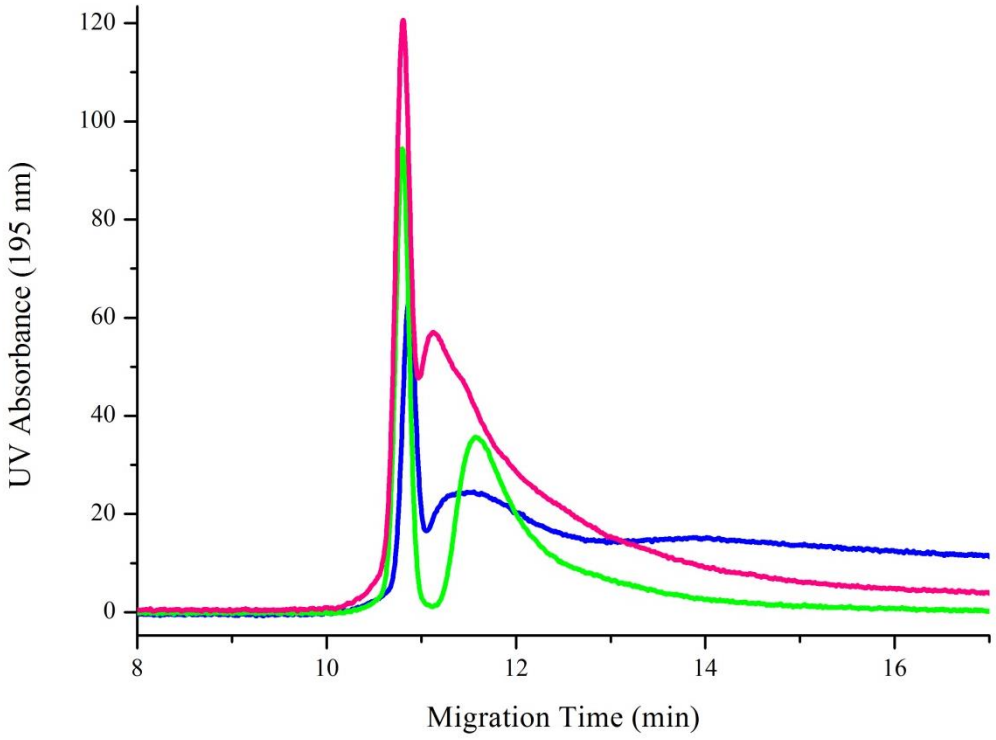

Figure S6. UV trace of pressure mobilization injections of linear PNaA (blue), 3-arm star PNaA (green) and hyperbranched PNaA (pink) in sodium phosphate buffer (10 mM) at pH 7.4 and 37 °C in a μSiL-WAX capillary displaying tailing peaks.

Results With a BGE at pH 9.2

Qualitative information on the interactions of serum with hyperbranched PNaA are given on Figure 1, and then on Figure S7 for the interactions with 3-arm star and linear PNaAs.

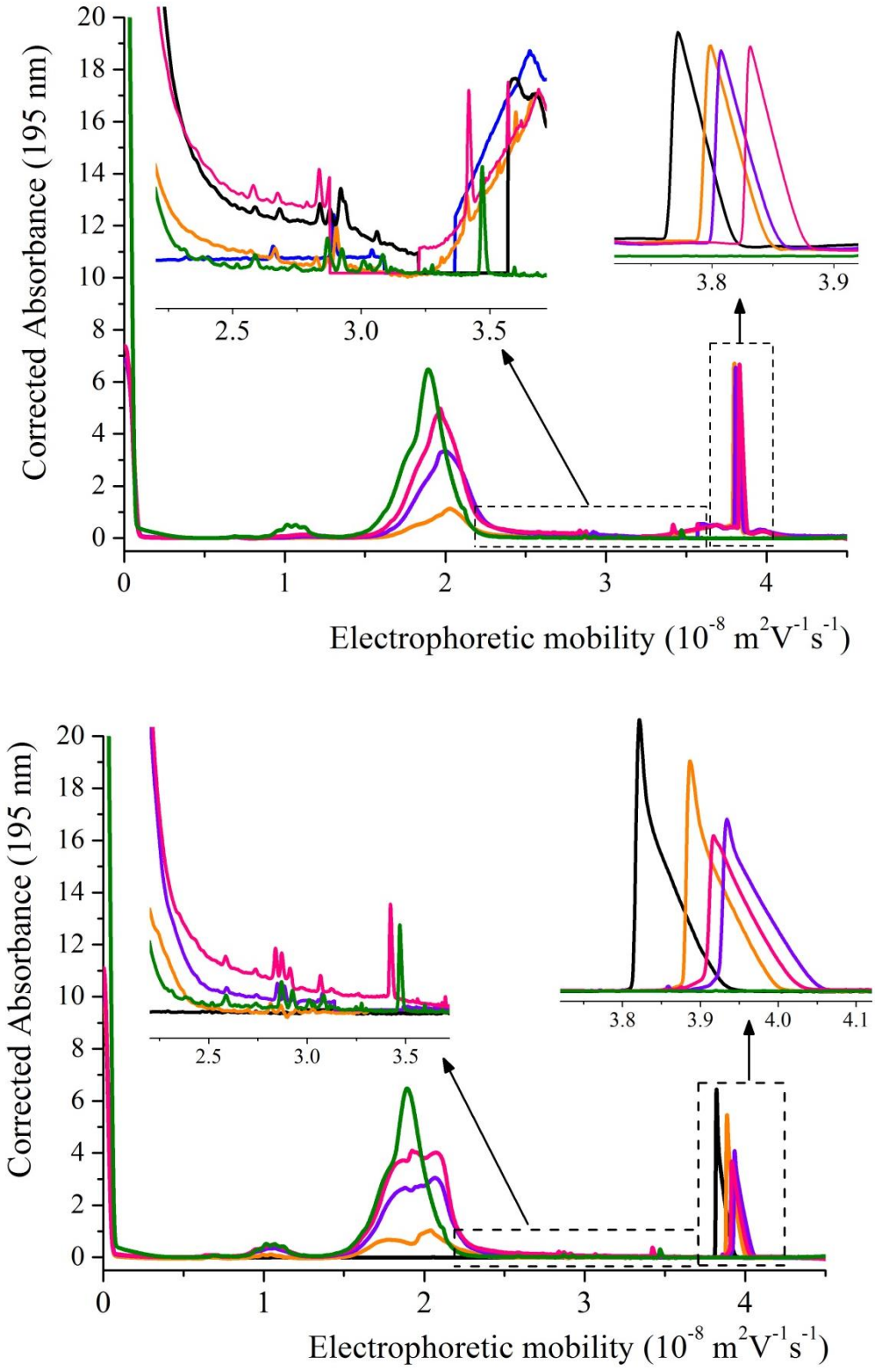

Figure S7. Electropherogram in the same conditions as Figure 1 of precipitated 3-arm star (top) and linear (bottom) PAA interaction with FBS: PNaA (black), FBS at 10 % (green), PNaA-FBS 2 % (orange), PNaA-FBS 5 % (purple) and PNaA-FBS 10 % (fuchsia). Insert shows the electrophoretic mobility of PNaA.

Hydrodynamic Radius of PAA Macromolecules

The hydrodynamic radius R_h was calculated according to Equation (S1) derived from the Flory expression for hydrodynamic volume and the Mark-Houwink-Sakurada relation:[4]

$$R_h = \left(\frac{3}{4\pi} \cdot \frac{K \cdot M^{\alpha+1}}{2.5 \times N_A}\right)^{1/3} \quad \text{(S1)}$$

where K and α are the Mark-Houwink-Sakurada parameters. The Mark-Houwink-Sakurada parameters for PAA in water were taken as $K = 1.53 \times 10^{-4}$ dL·g^{-1} and $\alpha = 0.786$.[5] The determined R_h values are listed in Table S.1.

Table S1. Hydrodynamic radii of PAA samples calculated from Equation (S1).

Architecture	**Molar Mass** [6] **[g·mol^{-1}]**	$\boldsymbol{R_h}$ **[nm]**
Linear PAA	39,300	1.6
3-Arm star PAA	8,500	0.6
Hyperbranched PAA	12,300	0.8

References

[1] D. C. Marks, L. Belov, M. W. Davey, R. A. Davey, A. D. Kidman, *Leuk. Res.* **1992**, *16*, 1165.

[2] B. G. Campling, J. Pym, P. R. Galbraith, S. P. C. Cole, *Leuk. Res.* **1988**, *12*, 823.

[3] M. Gaborieau, T. J. Causon, Y. Guillaneuf, E. F. Hilder, P. Castignolles, *Aus. J. Chem.* **2010**, *63*, 1219.

[4] E. Hosseini Nejad, P. Castignolles, R. G. Gilbert, Y. Guillaneuf, *J. Polym. Sci. A Polym. Chem.* **2008**, *46*, 2277.

[5] J. Bruessau, N. Goetz, W. Maechtle, J. Stoelting, *Tenside, Surfactants, Detergents* **1991**, *28*, 396.

[6] A. R. Maniego, D. Ang, Y. Guillaneuf, C. Lefay, D. Gigmes, J. R. Aldrich-Wright, M. Gaborieau, P. Castignolles, *Anal. Bioanal. Chem.* **2013**, *405*, 9009.